Sensor signal procesing

Quantum Approach to Image Data Encoding and Compression

Sathwik Reddy Majji[1*], Avinash Chalumuri[2*], and B. S. Manoj[3**]

[1] *Vikram Sarabhai Space Centre, Indian Space Research Organisation, Thiruvananthapuram 695022, India*
[2] *Gayatri Vidya Parishad College of Engineering, Visakhapatnam 530048, India*
[3] *Indian Institute of Space Science and Technology, Thiruvananthapuram 695547, India*
[*] *Member, IEEE*
[**] *Senior Member, IEEE*

Manuscript received 24 August 2022; revised 8 January 2023; accepted 22 January 2023. Date of publication 25 January 2023; date of current version 7 February 2023.

Abstract—High-resolution images are being generated due to the rapid development of image sensors. Various image processing algorithms require images of reduced sizes, given the computational constraints. Hence, preprocessing the images to reduce their size is crucial for many applications. This letter proposes a novel approach to compress images using quantum computing. A comparative study on different standard data encoding techniques used in quantum computing is undertaken. We propose four quantum compression techniques by extending the unitary operations of amplitude embedding for compressing images. The proposed methods provide exponential scaling as amplitude embedding is used, where 2^n classical data values are encoded into n qubits. Compression performance, visual evaluation, and objective evaluation are carried out to assess the proposed compression techniques. Our experimental results show that the crucial patterns in images are retained in the compressed images even at 75% compression. The compressed images can be used for postprocessing tasks using classical or quantum computing algorithms.

Index Terms—Sensor signal processing, data compression, data encoding, image processing, quantum circuit, quantum computing.

I. INTRODUCTION

Image sensors generate a large amount of data that are used for various real-time applications, such as classification and object detection [1]. However, extensive storage and computational facilities are required to store and process high-resolution images. Hence, traditional computational methods are sometimes insufficient. Quantum computing is a rapidly growing technology based on quantum-mechanical properties for computation [2], [3]. Classical computers can only encode data in bits that take a value of either 0 or 1, whereas quantum computers encode data in more than two states at a time using quantum-mechanical properties, such as superposition and entanglement. Thus, quantum computers are fundamentally different in processing information than classical computers.

A quantum bit or qubit is the basic unit of information in quantum computing. A qubit differs from a classical bit as qubits can be represented using a superposition of two basis states: $|0\rangle$ and $|1\rangle$. Hence, a qubit is a 2-D quantum system, and similarly, d-dimensional quantum systems (qudits) can be represented using the superposition of d basis states, such as $|0\rangle, |1\rangle, |2\rangle, \ldots, |d\rangle$.

As discussed earlier, analyzing high-resolution images requires storing and processing massive data. In addition, computational algorithms that handle large image data face complexity at training phase [4]. Quantum computing can solve the problem as quantum computers efficiently handle vast amounts of data by providing exponential scaling using qubits for computation [5].

This letter introduces a novel image data compression approach using quantum computing, where image data in the classical domain are encoded into a quantum computer for compression. The compressed image data in the quantum domain are later transformed into a downscaled image in the classical domain for desired postprocessing tasks. The main contributions of this letter are as follows:

1) We compared three existing quantum encoding techniques from the perspective of high-resolution imagery.
2) We proposed four quantum embedding methods using quantum circuits for image compression.
3) We experimented with the four methods on a dataset comprising 200 satellite images to reduce the size of the images.
4) We analyzed the effect of tuning the quantum circuits on the compressed image data using performance, visual, and objective evaluation methods.

II. DATASET AND DATA ENCODING TECHNIQUES

In this letter, we used a dataset of 200 satellite image tiles from [6] with less than 1% cloud coverage for the experiments. The chosen dataset has 100 pairs of synthetic aperture radar (SAR) (grayscale) and optical (RGB) images of the same area and taken at the same time. The 100 image pairs are split into two classes (50 image pairs each of airports and forestry). The selected satellite image tiles have a tile size of 1024×1024 pixels and a tile area of around 105 km^2.

Data encoding is essential in processing information using qubits on a quantum computer. The way of data encoding affects the efficiency of computational algorithms [7]. However, selecting a specific data encoding mechanism for high-resolution satellite images is an interesting research area. The properties of the data and the nature of the target remote sensing application are to be considered while selecting data encoding algorithms. The huge size of images is another consideration when selecting such a data encoding mechanism. Encoding image pixel data is the primary step in processing high-resolution satellite images. Embedding methods for data encoding are based on the following three standard techniques.

Corresponding author: B. S. Manoj (e-mail: bsmanoj@ieee.org)
Associate Editor: R. Vida.
Digital Object Identifier 10.1109/LSENS.2023.3239749

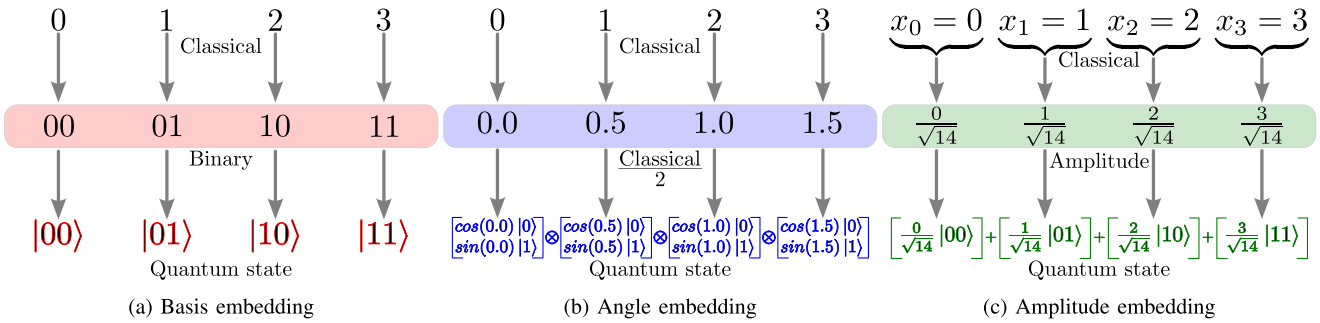

(a) Basis embedding (b) Angle embedding (c) Amplitude embedding

Fig. 1. Data encoding using the three standard qubit embedding techniques. (a) Basis embedding. (b) Angle embedding. (c) Amplitude embedding.

1) *Basis embedding:* In basis embedding [7], the classical data are converted to binary form; then, the string of binary inputs is translated as a quantum basis state, as shown in Fig. 1(a). The binary value of classical data is encoded as a basis state with an amplitude of 1. A classical data value with n binary bits is encoded using a basis state of n qubits in basis embedding. Thus, basis embedding requires many qubits to encode high-dimensional data because binary representations of the classical data are encoded as basis states.
2) *Angle embedding:* In angle embedding, classical data features are encoded as the rotational angles of qubits using unitary operations, as shown in Fig. 1(b). The qubit rotation can be achieved around x-axis $R_x(v^i)$ or y-axis $R_y(v^i)$ or z-axis $R_z(v^i)$ in a Bloch sphere [8], where v^i is the classical data value. The angle embedding encodes n classical features into a minimum of n qubits [7], where each feature is encoded as a rotational angle of a quantum rotational gate.
3) *Amplitude embedding:* In amplitude embedding, the classical features are mapped into amplitudes of a quantum state. The initial step in amplitude embedding is converting classical data into angular representations, as shown in Fig. 1(c). The data are encoded into amplitudes of quantum states using uniformly controlled rotations [9] as follows:

$$\left|\psi_{\text{amp}}\right\rangle = R\left(x_i, \beta\right)\left|k_1 k_2, \ldots ..., k_{s-2} k_{s-1}\right\rangle \left|k_s\right\rangle \tag{1}$$

where R is a function of x_i and β; x_i is the ith classical feature vector, and β is a parameter depending on the dimensions of the classical features [7]. State $|\psi_{\text{amp}}\rangle$ is the result of n rotations on the y-axis in a cascade, where n is the power for embedding a classical feature vector x_i. In general, to associate each amplitude with a component of the input vector, the dimension of the vector must be equal to a power of 2 because the vector space of an n-qubit register has dimension 2^n. After the rotations, the input vector $X = \{x_1, x_2, \ldots, x_n\}$ is encoded in the amplitudes of the quantum state as

$$|\psi\rangle = \sum_{i=0}^{n-1} x_i \,|i\rangle \tag{2}$$

where x_i is the normalized value of the ith classical feature.

A. Selection of Embedding Technique

Basis embedding is a primary way of encoding classical data using basis states. However, basis embedding encodes binary features into basis states; hence, the dimensionality and qubit requirement increases drastically. In angle embedding, a minimum of n qubits encodes n classical features. At present, noisy intermediate-scale quantum devices contain limited qubits to work with, and maintaining the coherence of many qubits is also a difficult task [10]. Hence, basis and angle embedding schemes are not the best choices for satellite images as encoding the classical data requires many qubits. In amplitude embedding, 2^n classical data features can be encoded using only n qubits. Since exponentially fewer qubits are required compared to other standard encoding techniques for data encoding, amplitude embedding is more suitable for satellite image data compression.

In this letter, we opted for a flexible approach where amplitude embedding followed by unitary operations is used as the quantum embedding method to encode and process satellite imagery. The unitary gates are meant for fine tuning the results.

III. QUANTUM COMPRESSION TECHNIQUES

This section discusses the four proposed quantum compression techniques (QCTs) using the amplitude embedding scheme followed by unitary operations to process and compress the remotely sensed image data. All four proposed compression techniques work on a four-wired quantum circuit that needs encoding of $2^4 = 16$ classical input parameters. The details of each QCT are provided as follows:

1) $\boldsymbol{QCT_1}$: In this compression technique, classical image pixel features (p) are encoded onto the four-wired quantum embedding circuit (QEC) using an amplitude embedding scheme (U_{amp}) with $|0\rangle$ as the initial state of all four qubits [11]. After encoding all the classical features into four qubits, the *Pauli-Z* measurement operator is used to measure the qubit values (q), as shown in Fig. 2.
2) $\boldsymbol{QCT_2}$: In this technique, encoding classical features (p) through U_{amp} is followed by *Pauli-X* operation at each wire, as shown in Fig. 2. The four wires after the *Pauli-X* operation are measured using *Pauli-Z* measurement operator.
3) $\boldsymbol{QCT_3}$: This technique starts in the same way as QCT_1 by encoding classical data p through U_{amp}. After the data encoding step, the information in the four wires is entangled with the help of three *CNOT* operations, as shown in Fig. 2. The four entangled wires are then measured using *Pauli-Z* measurement operator.
4) $\boldsymbol{QCT_4}$: This compression technique is a combination of QCT_1, QCT_2, and QCT_3, where the classical image pixel data (p) are encoded through U_{amp}. After encoding the data, each wire is subjected to *Pauli-X* operation, and the resulting qubits are then entangled with three CNOT operations, as shown in Fig. 2. The four entangled qubits are then measured using *Pauli-Z* measurement operator.

IV. EXPERIMENTS AND RESULTS

The experiments are conducted using the *PennyLane* [12] Python module. The chosen 200 SAR and optical images are downsized from

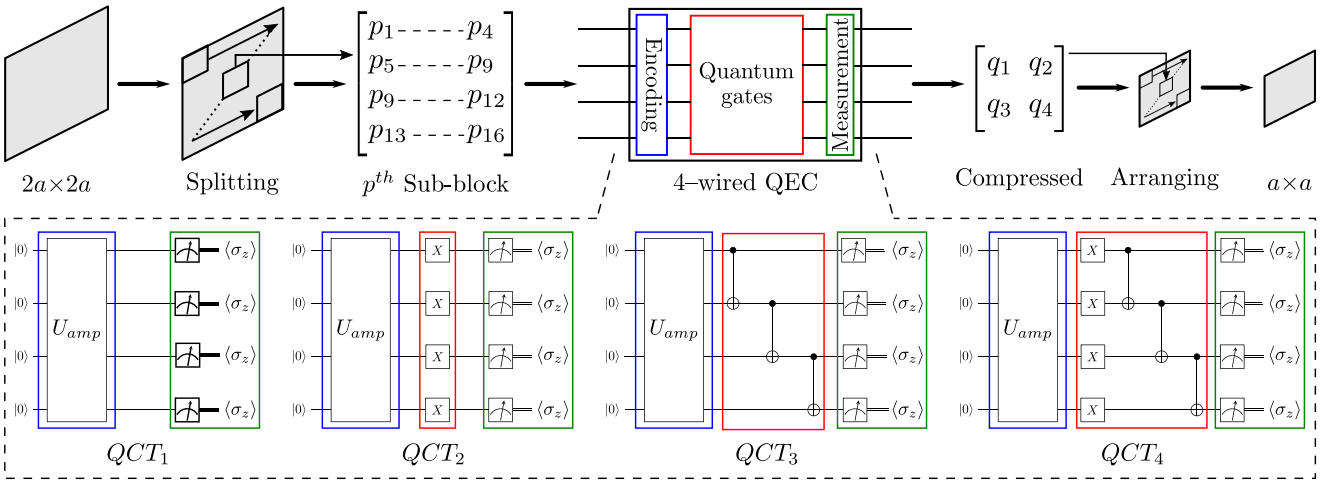

Fig. 2. Schematic diagram of the steps involved in high-resolution image processing.

1024×1024 to 400×400 due to the current limitation in the availability of quantum computational resources. First, each downsized image is split into subblocks containing 16-pixel data values, as shown in Fig. 2. The initial state of all the qubits is set to $|0\rangle$ by default, and the pixel values in each subblock ($p_1, p_2, \ldots, p_{16}$) are then encoded into a four-wired QEC by (U_{amp}) embedding scheme [11]. Later, a set of postencoding quantum gates further modifies the classical encoded data in the quantum domain. Finally, the modified quantum data are measured and converted back to the classical domain with a *Pauli-Z* measurement operator at the end of each wire. Since the work is with four wires, four measured values (q_1, q_2, q_3, and q_4) are obtained in the classical domain with each value between [–1, 1]. The measured values are scaled to [0, 255] for further processing. The resulting subblock is arranged to recreate a compressed image of 200 × 200, as shown in Fig. 2. Hence, this method theoretically compresses a subblock of 16 values to four values, resulting in 75% compression.

The effect of quantum gates in overall image compression can be studied with the four proposed techniques (QCT_1, QCT_2, QCT_3, and QCT_4). For this study, the compressed images are evaluated by three methods. The first is to analyze the four techniques based on their compression performance with the image dataset. The second is a visual analysis of the four techniques, which is a direct and commonly used evaluation approach. Since evaluating compressed images on visual interpretation is subjective, we have proceeded with the final evaluation method where the compressed images of all four techniques are objectively assessed with well-established quality metrics. The three evaluation methods to evaluate the proposed techniques are discussed as follows.

A. Compression Performance

As noted in the previous section, the theoretical data compression rate of the proposed four techniques is (16 pixels)/(4 values) = 4:1. However, a comparison with an actual image dataset is required for analyzing the four compression techniques. Hence, the average compression rates of the four techniques with SAR and optical image datasets are provided in Table 1. It is observed that the actual compression rates of the four proposed techniques are close to the theoretical value of 4:1. In addition, all the four techniques show a better compression rate with SAR images when compared to optical images. The enhanced performance for SAR images could be associated with the number of bands in an image since SAR images have one (grayscale) band compared to three bands (RGB) in the case of optical imagery. Even though the overall compression rates of all four techniques are close to 4:1, by comparing the compression rates of QCT_2 with QCT_1 and QCT_4 with QCT_3, it can be observed that the *Pauli-X* operation is impacting negatively in data compression performance. Another observation is that QCT_3 and QCT_4 compress better than the other two techniques implying that the entanglement of qubits through CNOT operation improves the compression rates.

Table 1. Compression Performance of the Proposed Techniques

Input data size (MB)	Compression technique	Output data size (MB)	Compression ratio (In:Out)
100 optical images with total size = 38.0502	QCT_1	10.7545	3.53807 : 1
	QCT_2	10.7545	3.53807 : 1
	QCT_3	10.6226	3.58200 : 1
	QCT_4	10.6590	3.56977 : 1
100 SAR images with total size = 13.3040	QCT_1	3.44506	3.86176 : 1
	QCT_2	3.44510	3.86171 : 1
	QCT_3	3.34790	3.97383 : 1
	QCT_4	3.36338	3.95554 : 1

B. Visual Evaluation

Fig. 3 shows eight sample SAR and optical image pairs, four from each class of the dataset, and their compressed images resulting from the four QCTs. Identifiable patterns are visible in all the compressed images. The compression of SAR imagery leads to distinguishable artificial structures, such as airport runways, taxiways, paths, and constructions. In contrast, the compression of optical imagery leads to better patterns in natural formations, such as fields around airports, terrain structures, water bodies, etc. Therefore, a fusion of these two compressed image pairs, as proposed in [13], would further enhance the image. In addition, images from QCT_1 and QCT_2 show better patterns when compared with images from the other two techniques.

C. Objective Evaluation

In this letter, four benchmark quality metrics are used for the objective evaluation of the compressed images. They are relative variance (RV) [13], peak signal-to-noise ratio (PSNR) [14], structural similarity index measure (SSIM) [13], and universal image quality

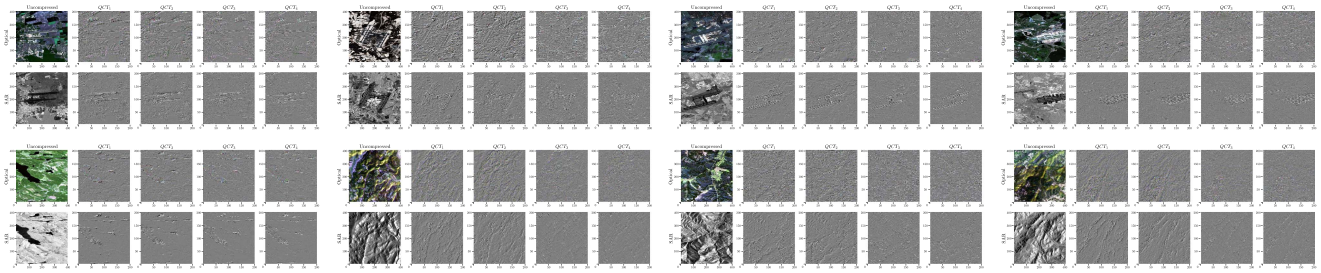

Fig. 3. Visual evaluation of eight selected SAR–optical image pairs and their compressed images resulting from the four QCTs.

Table 2. Objective Evaluation of the Compressed Images With Different Quality Metrics (Each Provided Value Is the Average of 200 Images)

Images	Technique	*RV*	*PSNR*	*SSIM*	*UIQI*
100 optical images	QCT_1	0.64595	17.6239	0.97959	0.67290
	QCT_2	0.64595	16.1442	0.97878	0.64452
	QCT_3	0.69528	16.9517	0.97870	0.66253
	QCT_4	0.69532	16.3907	0.97826	0.64825
100 SAR images	QCT_1	0.77409	17.3483	0.98976	0.84298
	QCT_2	0.77409	15.4930	0.98913	0.82017
	QCT_3	0.82938	16.7122	0.98943	0.83669
	QCT_4	0.82939	16.0712	0.98911	0.82641

index (UIQI) [15]. From Table 2, it is observed that the RV and PSNR values of compressed optical images are generally better than those of compressed SAR images implying a lower noise in compressed optical images. However, all the SSIM and UIQI values of compressed SAR images are better than those of compressed optical images. This indicates that though the compressed SAR images contain noise, they are structurally more similar and have greater quality than those of the compressed optical images. Comparing the RV values of QCT_1 and QCT_2 or QCT_3, and QCT_4 shows that the *Pauli-X* operation as a postencoding operation makes a little to no change in details of (or patterns in) images. However, comparing the PSNR, SSIM, and UIQI values of QCT_1 and QCT_2 shows that the *Pauli-X* operation alters the pixel intensity values of the compressed images. Another observation is that QCT_1 and QCT_3, in general, perform better than the other two techniques implying that postencoding entanglement of qubits is preferable over rotational quantum operations.

V. CONCLUSION

In this letter, we introduced a novel approach to compressing image data using quantum computing. Based on our approach, four QCTs were proposed and applied to compress a dataset of remotely sensed 200 SAR and optical images. The compression performance of the four QCTs was analyzed. Visual and objective evaluations were carried out to assess the compressed images. The results showed that the proposed techniques performed well at compression and were on par with the calculated theoretical value of compression. In addition, the crucial patterns in images were retained in the compressed images without significant loss of quality even when achieving about 75% compression.

The current limitation in the availability of qubits in real hardware forced the use of four-qubit quantum circuits in all the QCTs. The use of different quantum circuits is possible with the development and availability of additional hardware resources. The experiments are limited to a few sets of quantum gates, as this letter focused on introducing the possibility of quantum techniques for image compression. Further tuning of quantum circuits can be achieved to enhance image compression and quality. In addition, several classical or quantum algorithms can be designed to process the compressed images for various applications, such as training deep learning models for image classification.

REFERENCES

[1] P. Druzhkov and V. Kustikova, "A survey of deep learning methods and software tools for image classification and object detection," *Pattern Recognit. Image Anal.*, vol. 26, no. 1, pp. 9–15, Jul. 2016.

[2] A. Steane, "Quantum computing," *Rep. Prog. Phys.*, vol. 61, no. 2, Feb. 1998, Art. no. 117.

[3] L. Gyongyosi and S. Imre, "Advances in the quantum internet," *Commun. ACM*, vol. 65, no. 8, pp. 52–63, Jul. 2022.

[4] K. Simonyan and A. Zisserman, "Very deep convolutional networks for large-scale image recognition," 2014, *arXiv:1409.1556*.

[5] B. M. Terhal, "Quantum supremacy, here we come," *Nature Phys.*, vol. 14, no. 6, pp. 530–531, Jun. 2018.

[6] S. R. Majji, A. Chalumuri, R. Kune, and B. S. Manoj, "Data acquisition and utilization of quantum processed SAR and optical images for scene classification," *TechRxiv*, May 2022, doi: 10.36227/techrxiv.19672845.v2.

[7] M. Schuld and F. Petruccione, *Supervised Learning With Quantum Computers*, vol. 17. Berlin, Germany: Springer, 2018.

[8] O. Gamel, "Entangled Bloch spheres: Bloch matrix and two-qubit state space," *Phys. Rev. A*, vol. 93, no. 6, Jun. 2016, Art. no. 062320.

[9] M. Möttönen, J. J. Vartiainen, V. Bergholm, and M. M. Salomaa, "Transformation of quantum states using uniformly controlled rotations," *Quantum Inf. Comput.*, vol. 5, no. 6, pp. 467–473, Jun. 2005.

[10] J. Preskill, "Quantum computing in the NISQ era and beyond," *Quantum*, vol. 2, Aug. 2018, Art. no. 79.

[11] "qml.amplitudeembedding—Pennylane 0.25.1 documentation." Accessed: Aug. 22, 2022. [Online]. Available: https://docs.pennylane.ai/en/stable/code/api/pennylane.AmplitudeEmbedding.html

[12] V. Bergholm, J. Izaac, M. Schuld, C. Gogolin, and N. Killoran, "Pennylane: Automatic differentiation of hybrid quantum-classical computations," 2018, *arXiv:1811.04968*.

[13] S. R. Majji, A. Chalumuri, R. Kune, and B. S. Manoj, "Quantum processing in fusion of SAR and optical images for deep learning: A data-centric approach," *IEEE Access*, vol. 10, pp. 73743–73757, 2022.

[14] A. Horé and D. Ziou, "Image quality metrics: PSNR vs. SSIM," in *Proc. 20th Int. Conf. Pattern Recognit.*, 2010, pp. 2366–2369.

[15] Z. Wang and A. Bovik, "A universal image quality index," *IEEE Signal Process. Lett.*, vol. 9, no. 3, pp. 81–84, Mar. 2002.